Architecture and applications of drones for precision agriculture and environmental monitoring

University of Sannio

Laboratory of Signal Processing and Measurement Information, (LESIM)
Department of Engineering, University of Sannio, Benevento, Italy

Outline

- Introduction to drones
- General architecture of micro to small drones
- Drone applications for precision agriculture and environmental monitoring
- Technologies of sensors and measurement systems for precision agriculture and environmental monitoring

Drone development

Commercial Drones Are Set to Take Off

Forecasts vary, but anywhere from a quarter-million to a million-and-a-half working drones will enter U.S. skies in the next four years.

COMMERCIAL DRONES DEPLOYMENT FORECAST

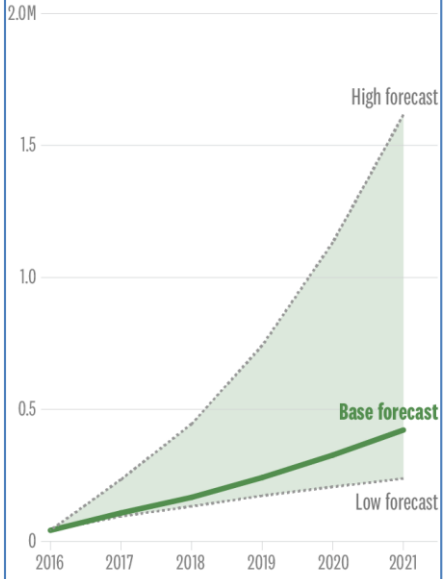

SOURCE FAA © HBR.ORG

The Three Waves of the Drone Economy

MARKET EVOLUTION

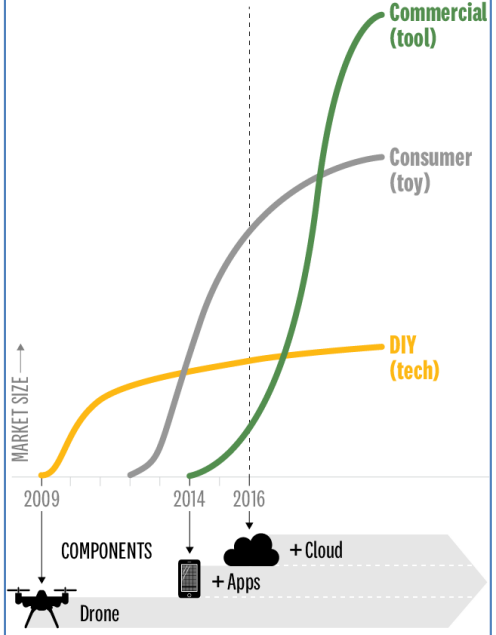

SOURCE CHRIS ANDERSON © HBR.ORG

Jobs for Drones

As more industries look at drone technology, the list of jobs drones can do—or could do—is growing. But what's real?

DEVELOPMENT STAGE

Early	Mid	Late
Mail/small package delivery	Construction/ real estate images and monitoring	Aerial photography
	Emergency management	Border patrol
	Filmmaking/ other media	Precision agriculture
	Infrastructure monitoring	Public safety
	Oil and gas exploration	
	Weather forecasting/ meteorological research	
	Wildlife/ environmental monitoring	

SOURCE "DRONE INDUSTRY REPORT," OPPENHEIMER & CO., FEBRUARY 2016 © HBR.ORG

Reality capture

- **“Reality capture”** is the process of digitizing the physical world by scanning it inside and out, from the ground and the air.
- Example: In Google Maps, data was captured by satellites, airplanes, and cars, and presented in 2-D and 3-D maps.
- Now that kind of mapping, initially designed for humans, is done at much higher resolution in preparation for the self-driving car.

http://www.atlatec.de/en/

Drones for reality capture

- Industries have long sought data from above, generally through satellites or planes, but drones are better "**sensors in the sky**" than both.
- They gather higher-resolution and more-frequent data than satellites (whose view is obscured by clouds over two-thirds of the planet at any time), and they're cheaper, easier, and safer than planes.
- Drones can provide "anytime, anywhere" access to overhead views with an **accuracy** that rivals laser scanning.

SYSMAP SenseFly

Accuracy of drone measurements

- Drones have been recently proposed to map the scene of car accidents.
- In all cases when economic transactions or legal issues are involved, it is fundamental to provide the uncertainty of the measurement result through structured and traceable procedures.
- Image data collected during the drone flight can be used to produce a 3D point cloud and distance and size measurements, with **unofficial and approximate accuracy** of 2-5 cm.

What is a drone?

- **Aircraft:** Any machine that can derive support in the atmosphere from the reactions of the air other than the reactions of the air against the earth's surface
- **Autonomous aircraft:** An unmanned aircraft that does not allow pilot intervention in the management of the flight
- **Remotely-piloted aircraft:** An aircraft where the flying pilot is not on board the aircraft
- **Remotely-piloted aircraft system:** A set of configurable elements consisting of a remotely-piloted aircraft, its associated remote pilot station(s), the required command and control links and any other system elements as may be required, at any point during flight operation.

Unmanned aircrafts

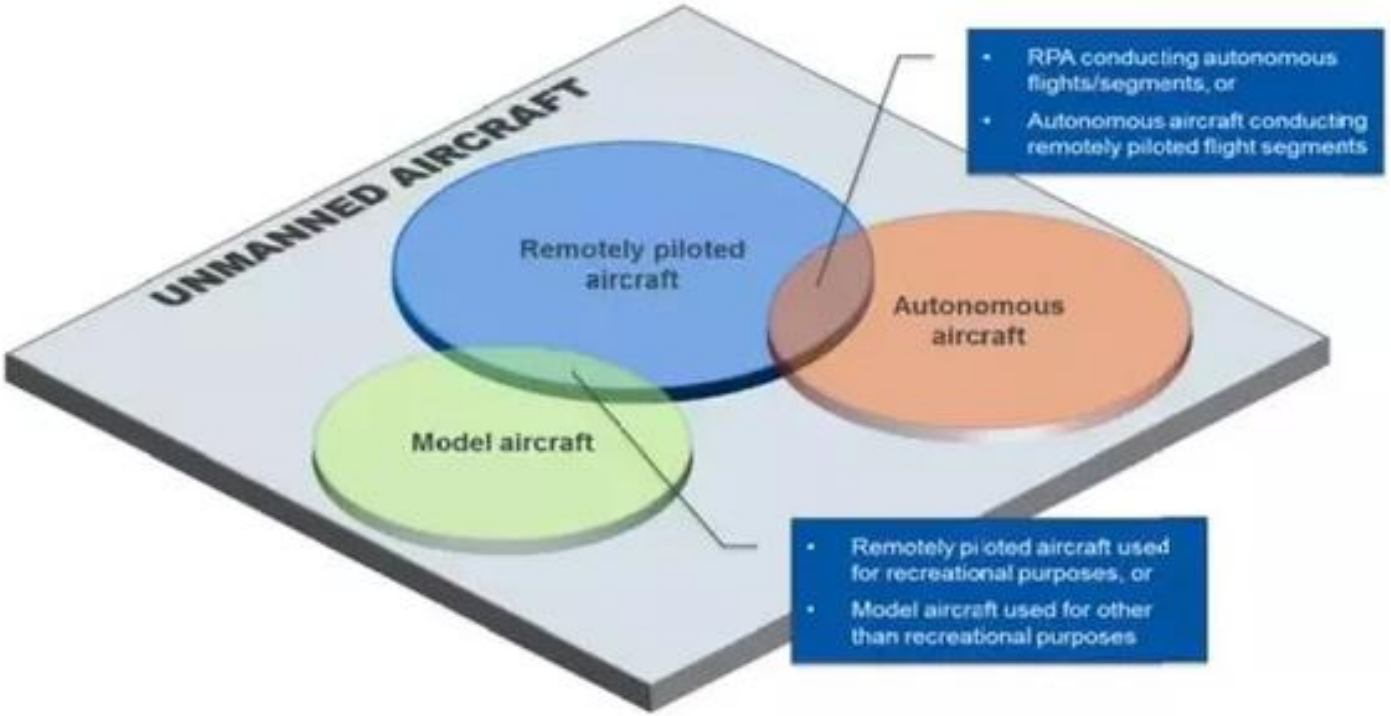

Classification of drones

Number	Mean take-off weight (MTOW)	Name
0	Less than 1 kg	Micro
1	Up to 1 kg	Mini
2	Up to 13.5 kg	Small
3	Up to 242 kg	Light/ultra light
4	Up to 4332 kg	Normal
5	Over to 4332 kg	Large

MTOW is proportional to the expected kinetic energy imparted at impact.

Drones we will refer to…

- MTOW < 13.5 kg;
- Vertical Take-Off Landing (VTOL);
- Very low altitude (VLA), 150 m;
- Operations in line-of-sight (*LOS*) and beyond-line-of-sight (*BLOS*)
- Remotely operated (semi-autonomous): the drone can perform high-level commands (waypoints, objects tracking, etc.), and its performance is monitored by a trained operator.

https://www.dji.com/

General architecture of a micro to small drone

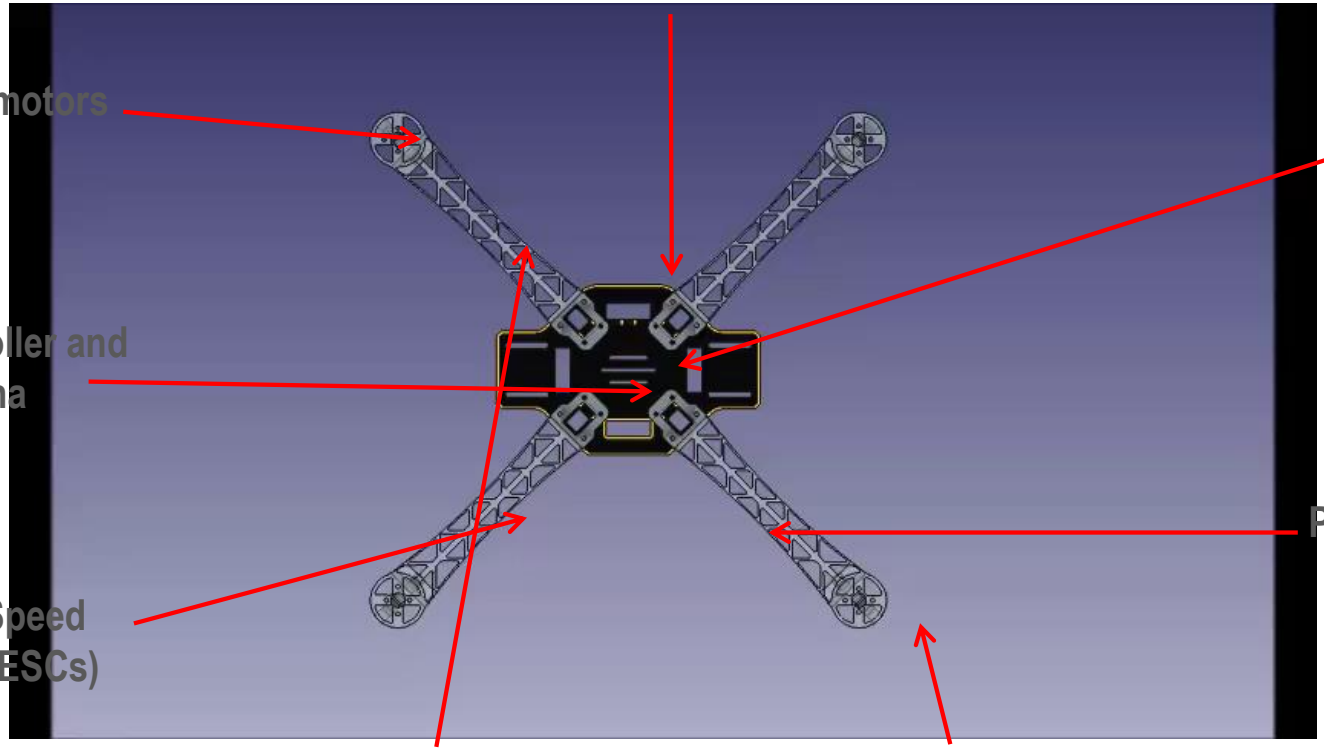

Sensors of drones

Sensors for navigation

Sensors for mission

Drone electronics

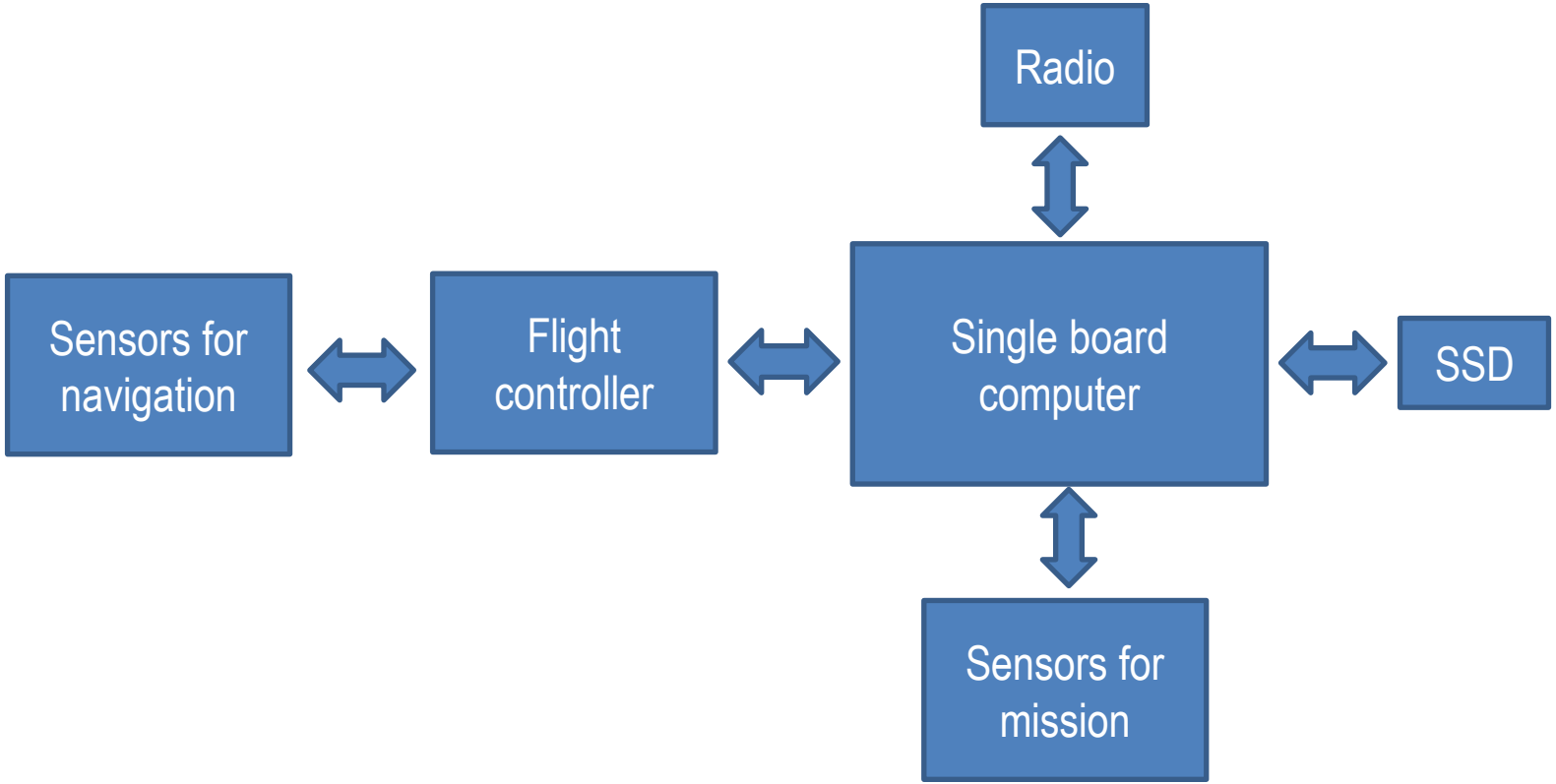

Software architecture

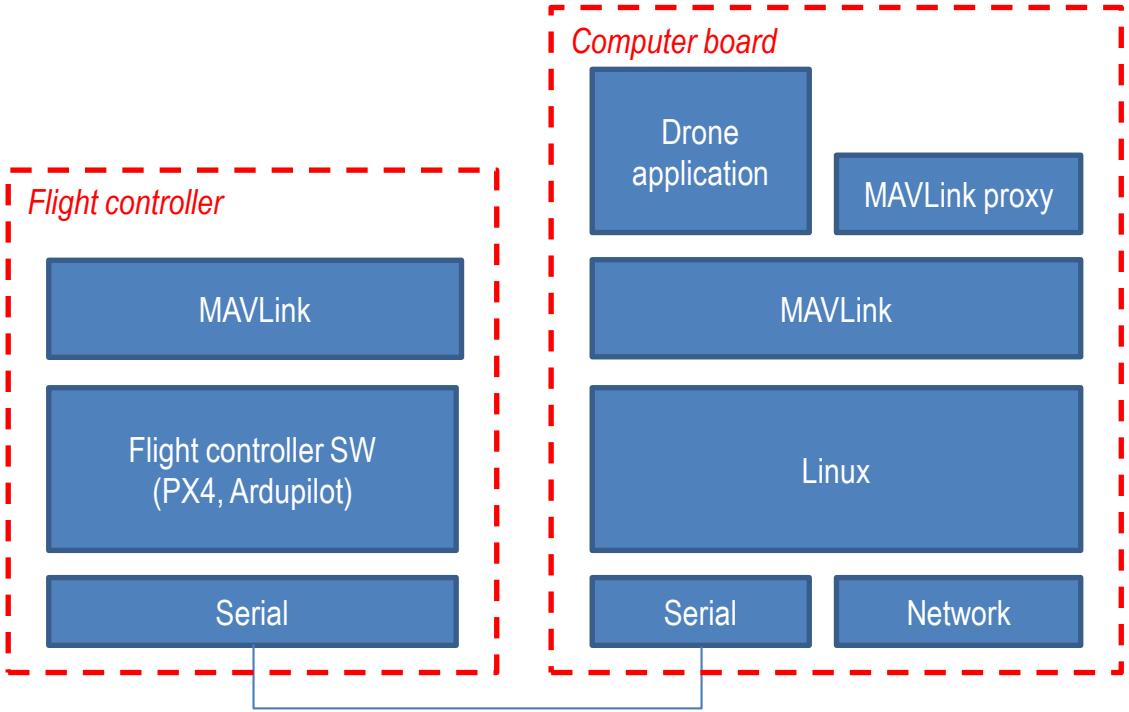

MAVLINK
MICRO AIR VEHICLE COMMUNICATION PROTOCOL

MAVLINK
(Micro Air Vehicle Link) is an industry-standard protocol for communicating with flight controllers

Ground control station

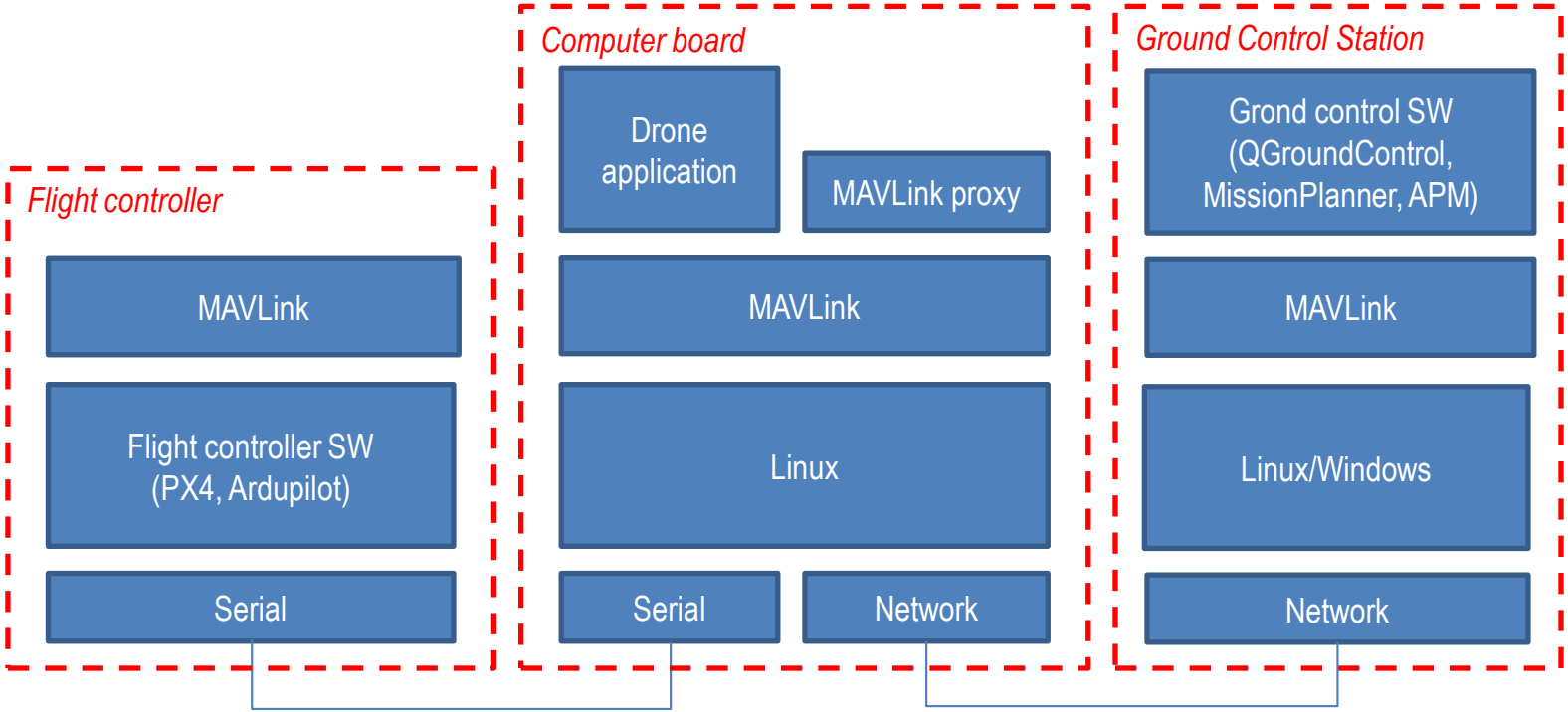

Drone-based instrument

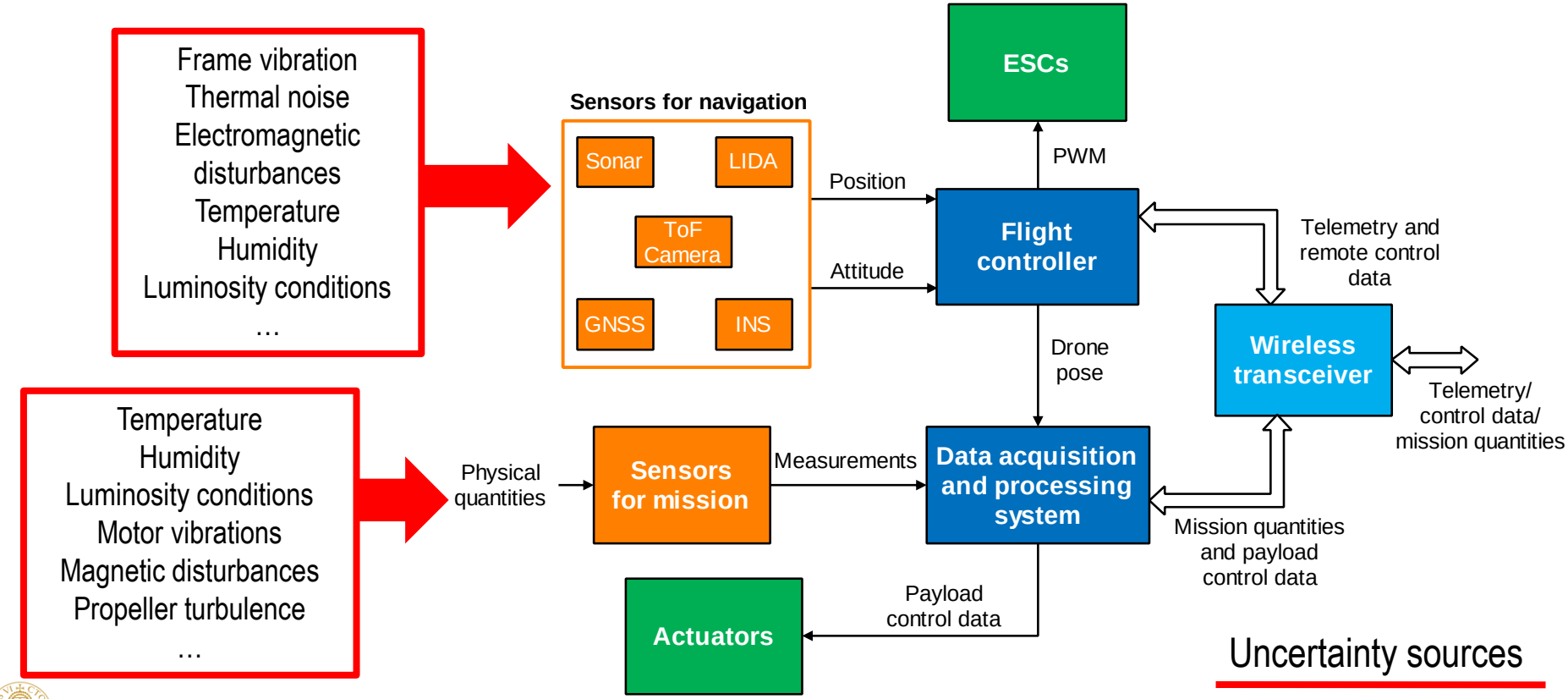

Drone applications in agriculture and forestry (1/2)

- The use of drones in agriculture has recently been introduced for big areas inspection and smart targeted irrigation and fertilization.
- The possibility of detecting the areas where a major irrigation is needed or where a foliage disease is spreading, can help agronomists to save time, water resources and reduce agrochemical products. At the same time, such advanced farming techniques may lead to increased crop productivity and quality.

Drone applications in agriculture and forestry (2/2)

It is possible to classify two main types of applications for precision agriculture and forestry according to the sensors embedded on drones:

- Applications based on multi- and hyper- spectral cameras
- Applications based on RGB cameras

Detection of aquatic weeds

- The Centre for Regional and Rural Futures (CeRRF) at Deakin University (Australia) has been using drones with multispectral sensors to identify and monitor aquatic weeds in irrigation systems.
- Early detection is key since aquatic weeds can impact farm productivity by disrupting the irrigation flow.

Tree classification and forest monitoring

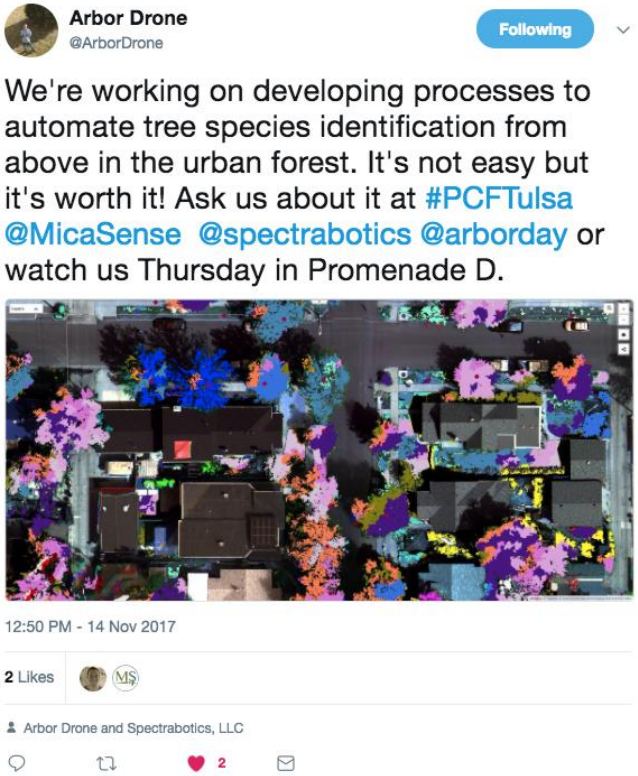

- The spectral signature of trees can be used to detect and classify them from multispectral images.
- This can help tree species identification and forest monitoring.

Observing variation in time

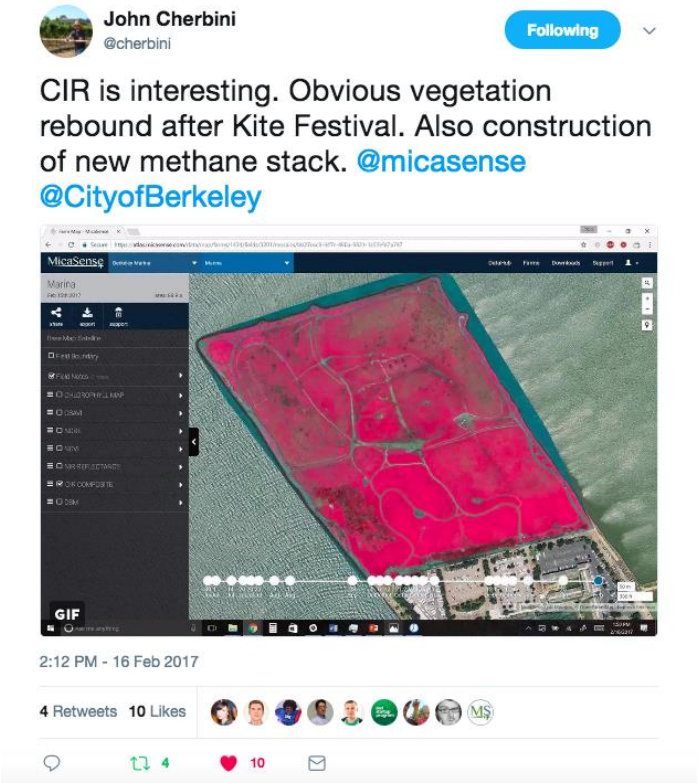

- Data from different flights are analyzed over the same field
- It is possible to compare how the indices values changed over time to detect variation.

Vegetation monitoring

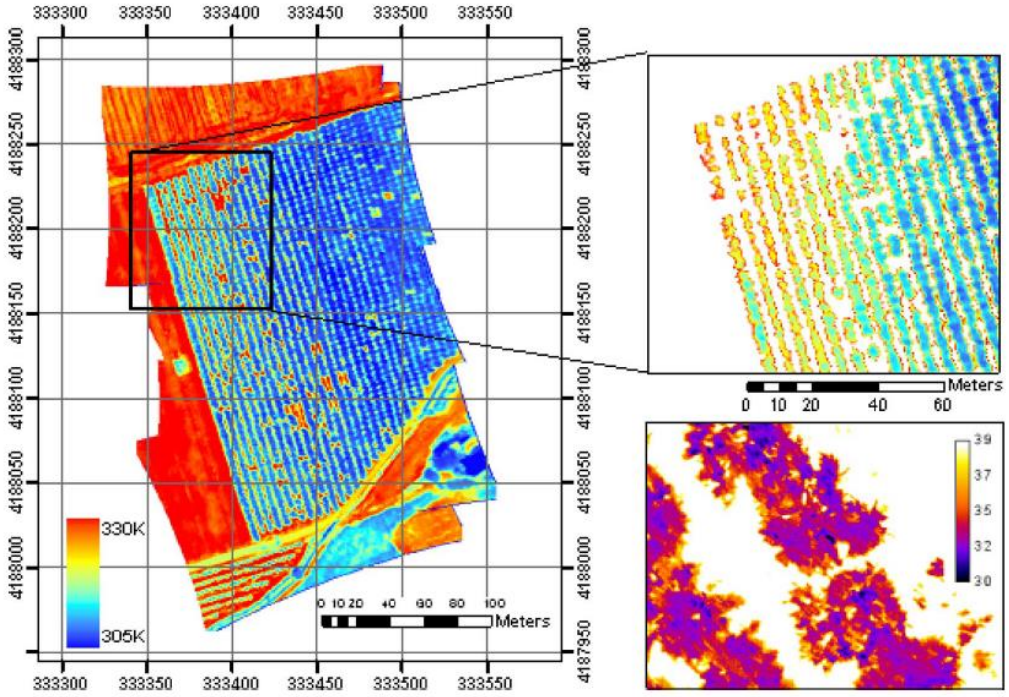

Infrared image, to analyze water needs of plants.

Estimation of chlorophyll concentration and Leaf Area Index from multispectral images

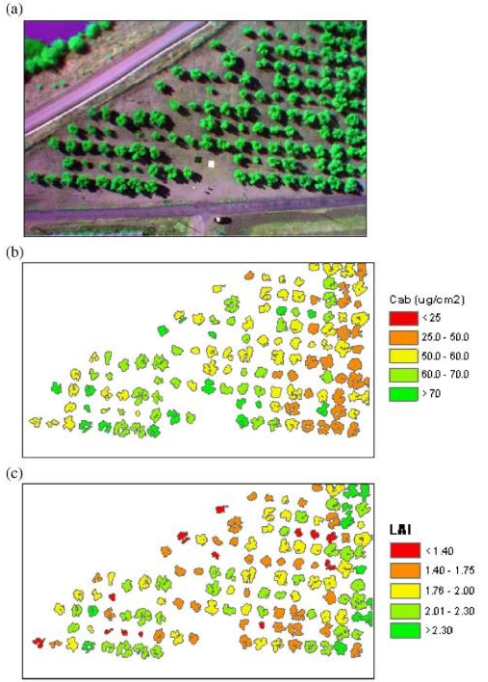

3D Canopy of a vineyard

DSM extracted from drone pictures

Subtracting DTM from DSM to obtain the canopy profile

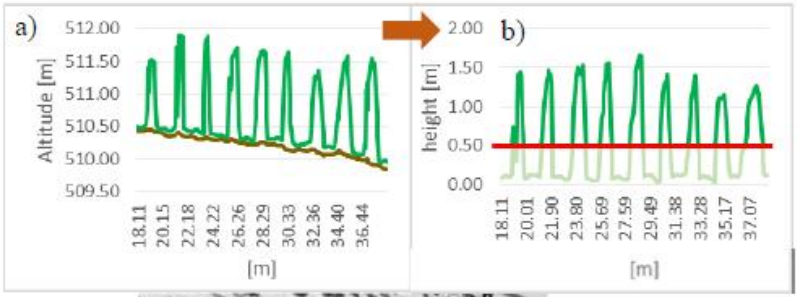

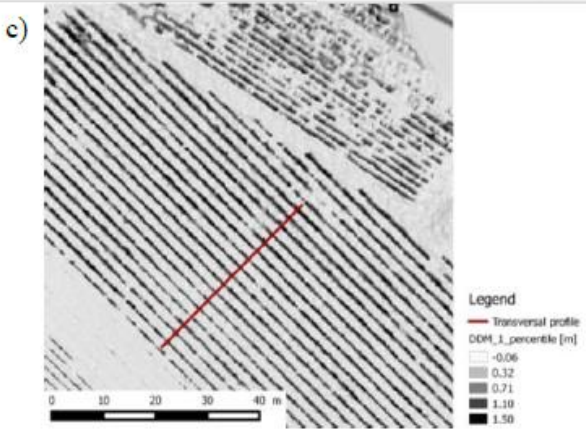

3D forest canopy model

Measurements by multi- and hyper- spectral cameras

- The drone sensors simultaneously sample spectral wavebands over a large area
- After post-processing, each pixel in the resulting image contains a sampled spectral measurement of the reflectance, which can be used to identify the material present in the scene.
- From the reflectance measurements, it is possible to quantify the chlorophyll absorption, pesticides absorption, water deficiency, nutrient stress or diseases

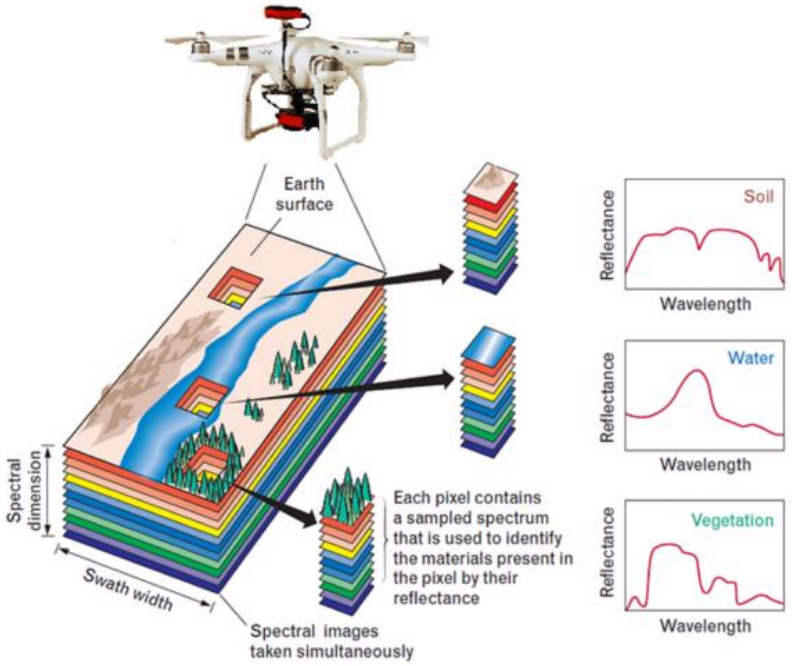

Fundamental of spectral imaging

Irradiance refers to the light energy per unit time (power) impinging on a surface, normalized by the surface area, and is typically specified in watts per square meter (W/m^2);

Reflectance is a unitless number between 0 and 1 that characterizes the fraction of incident light reflected by a surface. Reflectance may be further qualified by parameters such as the wavelength of reflected light, the angle of incidence, and the angle of reflection.

Radiance is simply the irradiance normalized by the solid angle (in steradians) of the observation or the direction of propagation of the light, and is typically measured in W/m^2/steradian.

Normalizing the radiance by the wavelength of the light, which is typically specified in μm, yields **spectral radiance**, with units of W/m^2/μm/steradian.

Reflectance Spectrum (1)

The color and reflectivity of an object are typically important indications of the material composition of the object, since different materials absorb and reflect the impinging light in a wavelength-dependent fashion.

The reflected light or spectral radiance $L_S(\lambda)$ that a sensor records is given by:

$$L_S(\lambda) = \rho(\lambda) L_i(\lambda)$$

where $L_i(\lambda)$ is the impinging scene radiance and $\rho(\lambda)$ is the reflectance spectrum of the material.

By knowing $L_i(\lambda)$, the reflectance spectrum can be recovered.

Reflectance Spectrum (2)

- Since the reflectance spectrum is independent of the illumination, the reflectance spectrum provides the best opportunity to identify the materials in a scene by matching the scene reflectance spectra to a library of known spectra.
- In the case of solar illumination, the spectral irradiance of the light reaching the atmosphere is reasonably well characterized.
- The recovery of reflectance spectra of different objects and materials must take into account the effects the atmosphere has on the spectrum of both the solar illumination and the reflected light.

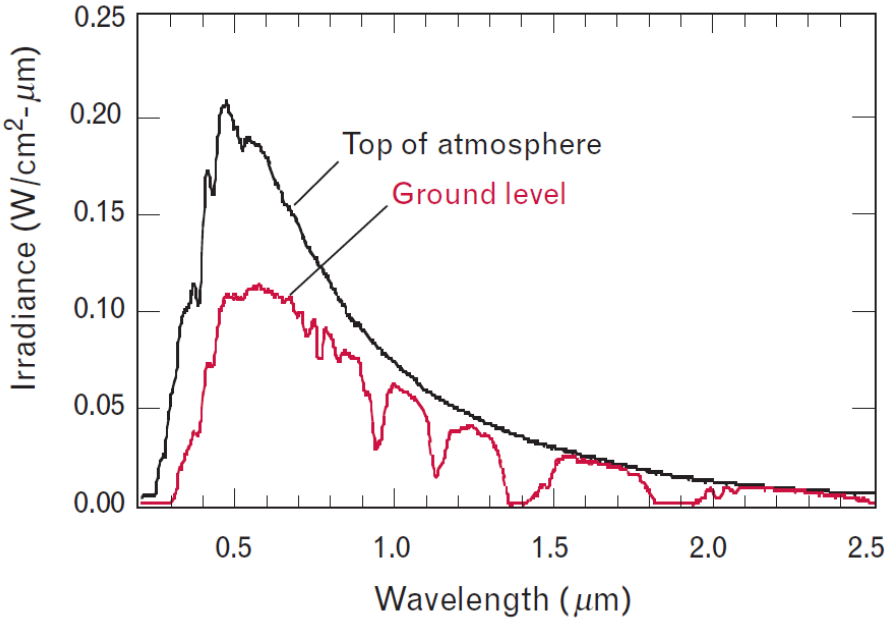

Hyperspectral camera

Push-broom imaging sensor

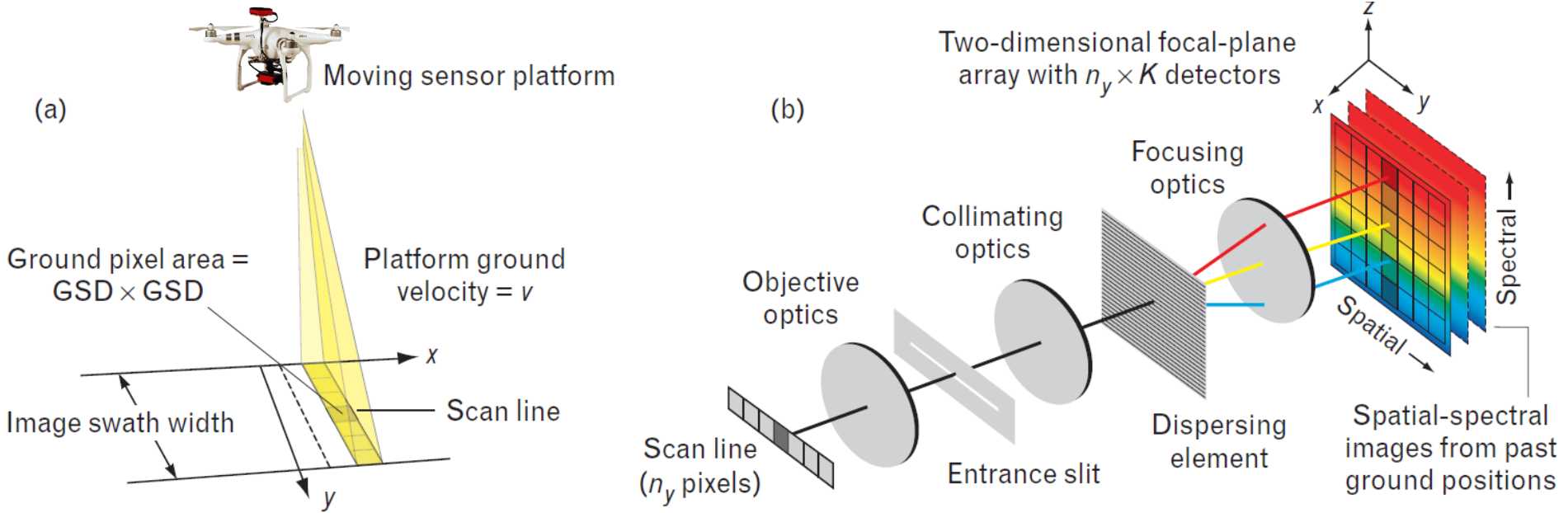

Multispectral camera

Sensors based on multiple cameras

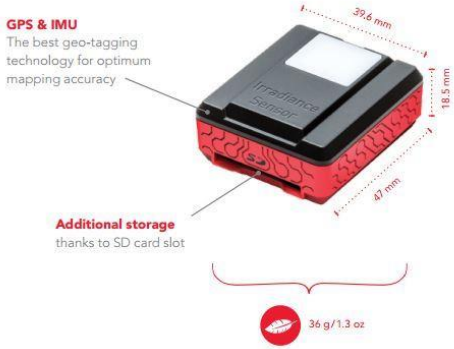

To cope with light variability, Sequoia incorporates a second sensor, known as an irradiance sensor. It is mounted on the back of the drone.

During the flight it will continuously sense and record the light conditions in the same spectral bands as the multispectral sensor.

Sampling with multispectral cameras

There are four sampling operations involved in the collection of spectral image data:

Spatial sampling;

Spectral sampling;

Radiometric sampling;

Temporal sampling.

Spatial sampling: Ground Sample Distance (GSD)

The GSD is the distance on the ground that is covered from each pixel of the camera sensor embedded on drone.

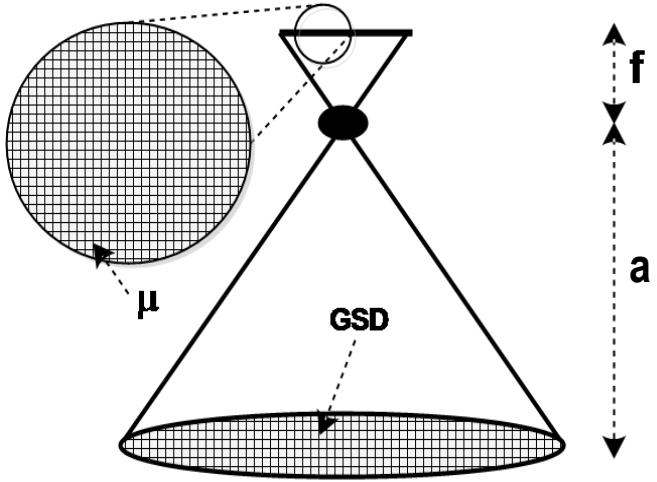

$$\mathrm{GSD} = \frac{a}{f} \cdot \mu$$

- *a* is the flight altitude
- *f* is the camera focal length
- *μ* is the pixel size

By reducing the flight altitude, the GSD value reduces but the required time for the survey increases.

Pratical considerations

Reducing the aperture size reduces sensor cost but results in degraded spatial resolution (i.e., a larger GSD).

For a spectral imager, the best detection performance is expected when the angular resolution of the sensor, specified in terms of the GSD, is commensurate with the footprint of the targets of interest.

By reducing the flight altitude of the drone the GSD becomes lower, but the mission time required for the survey of the area increases.

Spectral sampling

Spectral sampling is achieved by decomposing the radiance received in each spatial pixel into a number of wavebands.

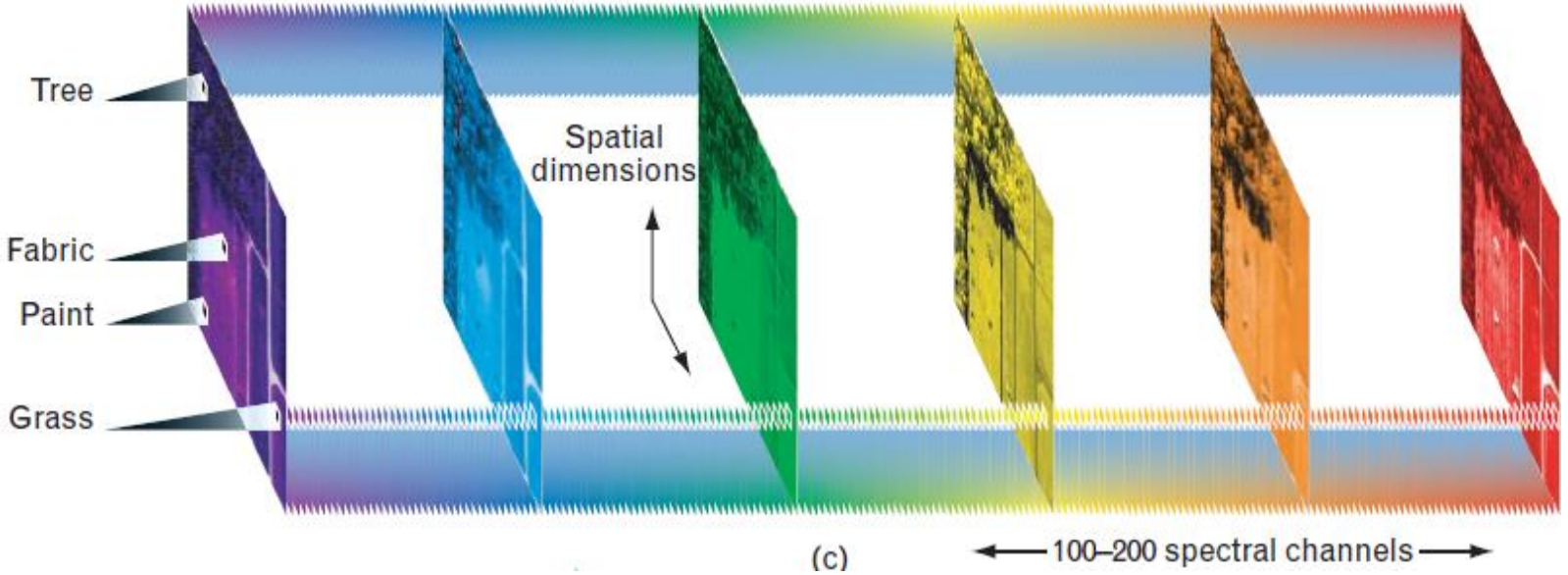

Radiometric sampling

An analog-to-digital converter samples the radiance measured in each spectral channel, producing digital data at a prescribed radiometric resolution.

Temporal sampling

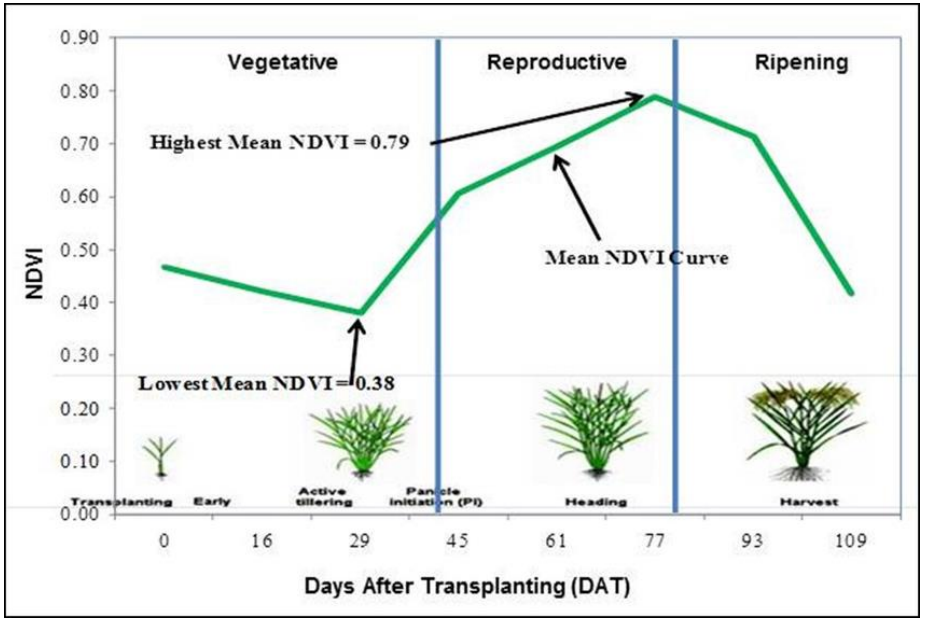

The term temporal sampling does not refer to the time associated with image formation, but to the process of collecting multiple spectral images of the same scene separated in time.

Temporal sampling is an important mechanism for studying natural and anthropogenic changes in a scene.

Atmospheric Effects (1)

- The atmosphere modulates the spectrum of the solar illumination before it reaches the ground.
- This modulation must be known or measured in order to separate the spectrum of the illumination (the impinging solar radiance) from the reflectivity (the reflectance spectrum) that characterizes the materials of interest in the scene.

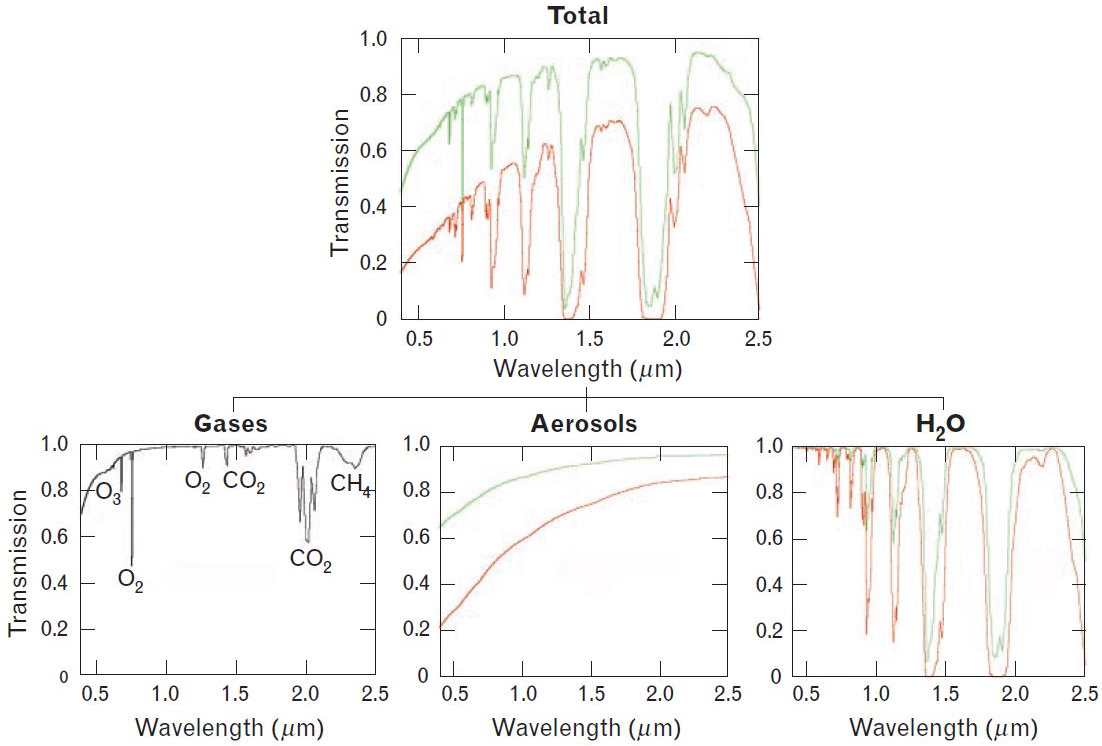

Atmospheric Effects (2)

- The solar radiation is scattered by the atmosphere into the field of view of the sensor without ever reaching the ground. This scattered light is superimposed on the reflected light arriving from the scene, and is termed path radiance because it appears along the line-of-sight path to the scene.
- The solar radiation scattered by the atmosphere, predominantly in the blue region of the visible spectrum, acts as a secondary source of diffuse colored illumination. This diffuse sky illumination is most important for shadowed objects, since regions shadowed from the direct rays of the sun may still be illuminated by the diffuse non-white sky radiation.
- The solar illumination that reaches the scene and is reflected by the target is further absorbed and scattered by the atmosphere as it propagates toward the sensor.

Compensation of the atmospheric effects

The methods for compensating the atmospheric effects can be classified in:

- scene-based statistical methods;
- physics-based modeling methods.

Scene based statistical methods

They use a-priori knowledge of the reflectance characteristics of specific reference objects (such as calibration panels) in a scene to develop statistical relationships between the at-sensor observations and the known surface reflectance.

Calibration reference panel for NIR

The empirical line method (ELM) is one of the oldest and most commonly used statistical methods for atmospheric compensation

The empirical line method (1)

The reference objects are selected or constructed to provide relatively constant reflectance over the spectral measurement bands of interest.

1. Field measurements of the surface reflectance of selected reference objects are made on the ground, at close range, under controlled conditions.
2. The reference objects are positioned in the scene to ensure good line-of-sight visibility to the drone platform.
3. During data collection, these reference objects are included in the imagery collected by the sensor.
4. For each spectral band in the sensor data, a linear regression is performed to relate the measured radiance to the corresponding ground reflectance of the reference objects.

The empirical line method (2)

5. Field measurements of the surface reflectance of the selected reference objects are made on the ground, at close range, under controlled conditions.
6. The gain-offset correction factors for each spectral band are estimated.

For example:
Data containing two reference reflectance objects, one a nominal 4% reflectance panel and the other a nominal 32% reflectance panel.
The average radiance for all the pixels in a given panel is plotted against the ground reflectance measurement.

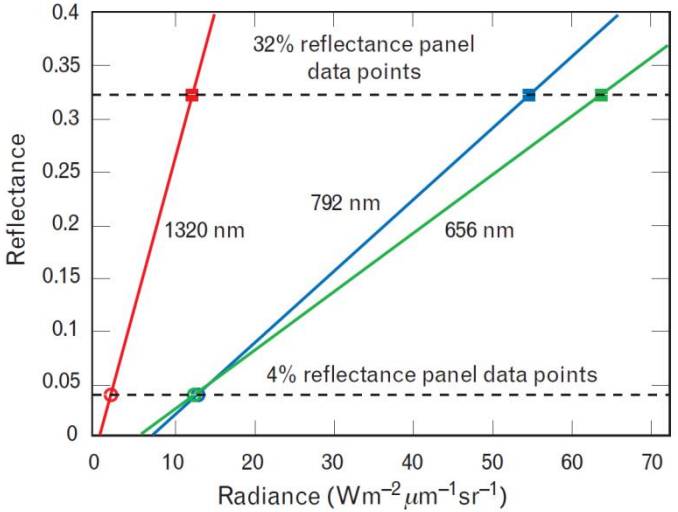

The empirical line method (3)

7. Given a sensor radiance measurement $L_s(\lambda)$, and the gain and the offset, $\mathrm{G}(\lambda)$ and $L_0(\lambda)$, terms the reflectance $\rho(\lambda)$ can be obtained with the following formula:

$$\rho(\lambda) = \frac{L_s(\lambda) - L_0(\lambda)}{\mathrm{G}(\lambda)}$$

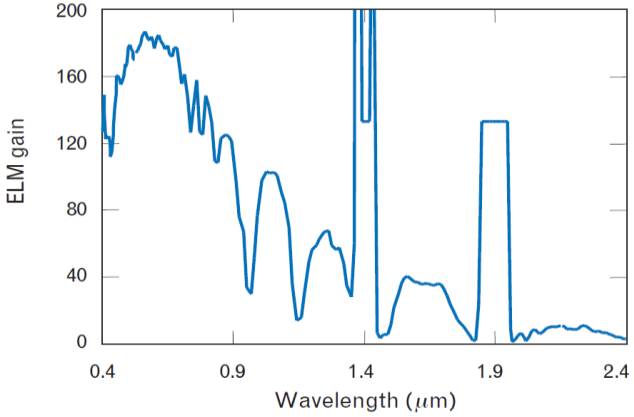

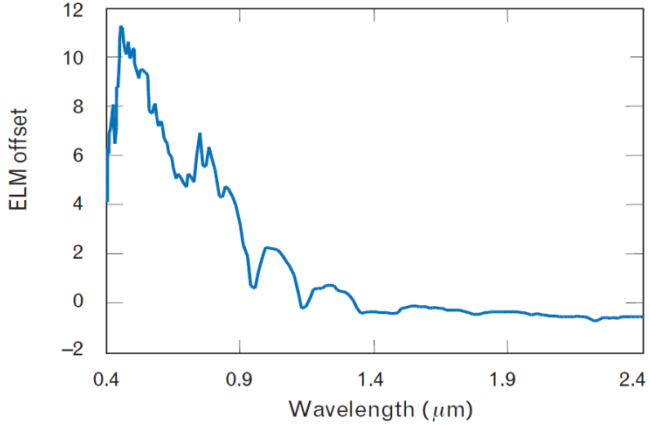

Physics-based modeling methods

Fast line-of-sight atmospheric analysis of spectral hypercubes (FLAASH)

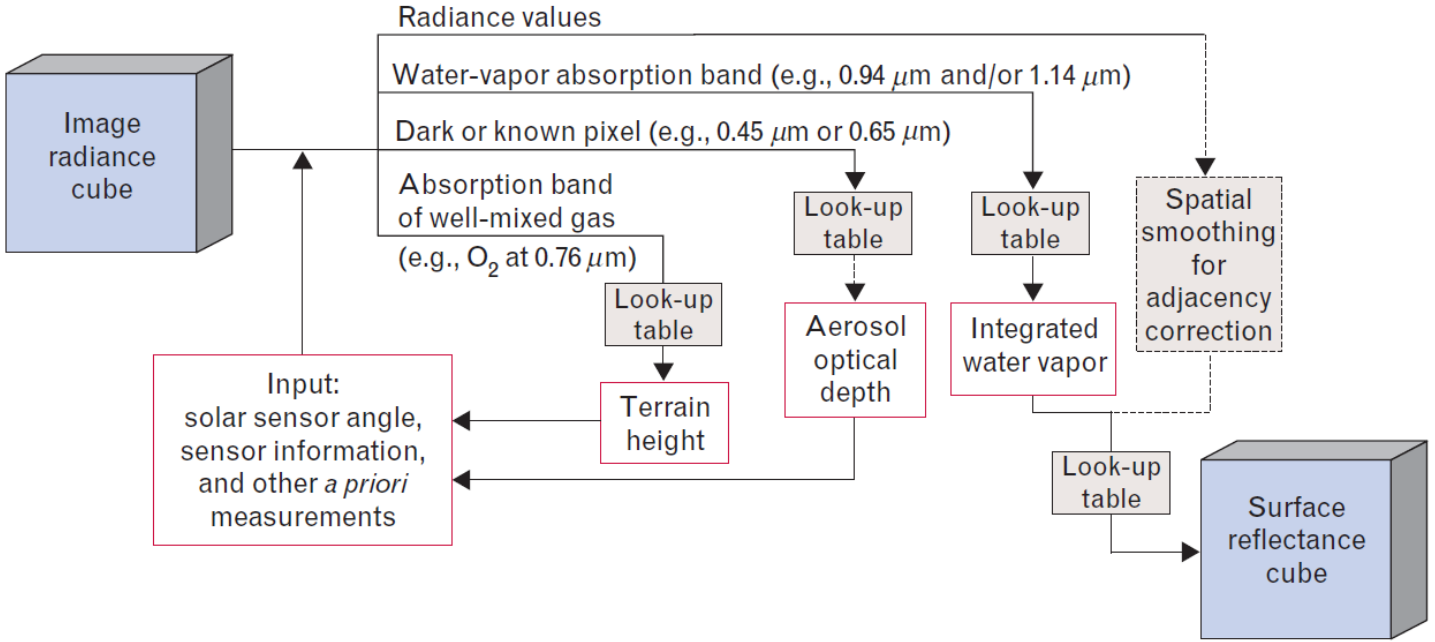

3D reconstruction with RGB cameras

The images acquired by drones embedding RGB cameras are used to obtain the 3D reconstruction of the surveyed area.

The 3D reconstruction is implemented by means of structure from motion, consisting in acquiring two consecutive images during the flight mission

From the 3D reconstruction, Digital Terrain Models and Digital Surface Models are extrapolated.

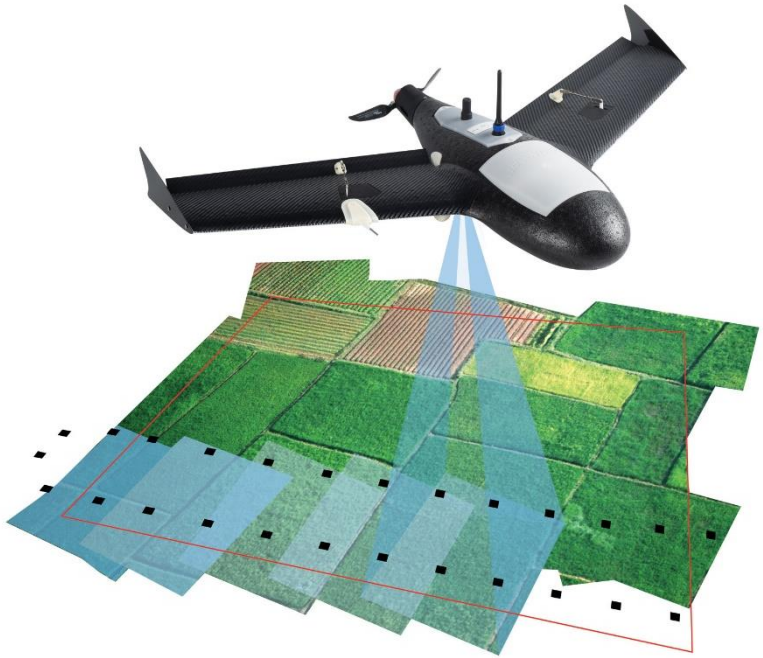

Stereo-vision system

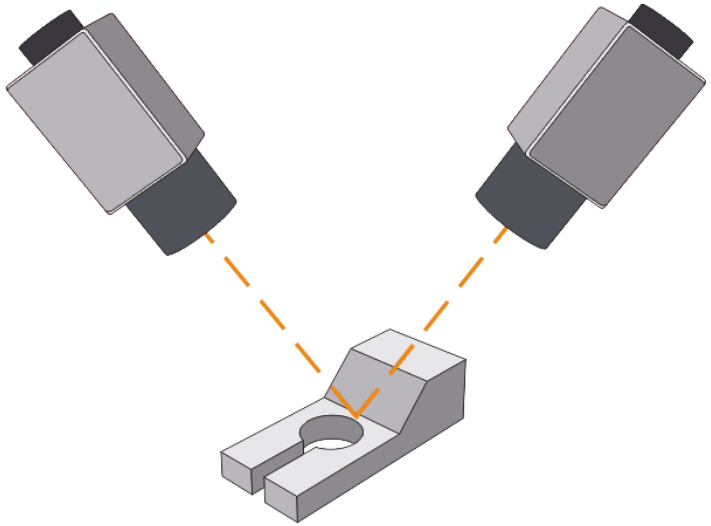

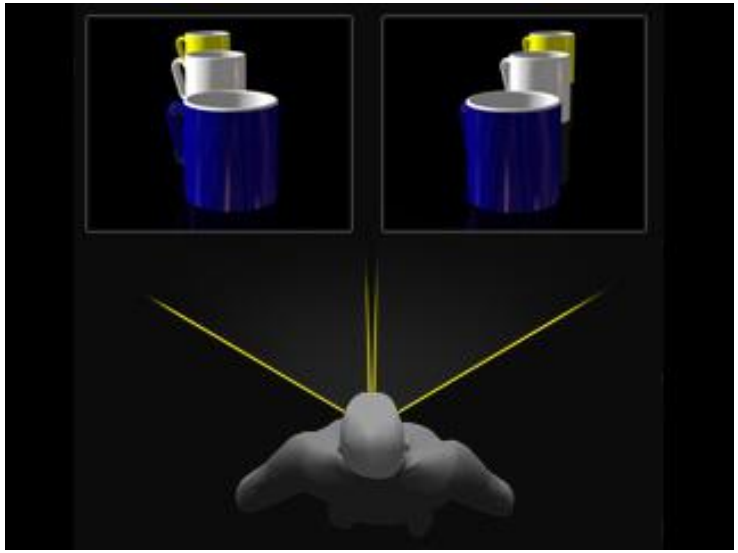

The aim of a stereo vision system is to provide measurements related to the width, the height and the **depth** of an object.

Stereo-vision: measurement procedure

- Stereo-vision system calibration: by using reference targets, it is possible to estimate the projection matrices of the actual object to the images;
- Recognition of the projections of the observed point on both the left image and the right image (stereo matching). The recognition of the same point projected on the two images requires the implementation of image processing algorithms for the detection of common features on both of them;
- Given the points of the observed point on both images and by knowing the projection matrices estimated in the previous step, it is possible to determine the coordinates of the observed point in the absolute reference coordinate system (scene structure or triangulation).

Depth estimation

$$z = \frac{bf}{x'_L - x'_R} = \frac{bf}{d}$$

If the disparity value is low, the uncertainty value of the disparity increases and the uncertainty related to the z estimation increases.

For decreasing the disparity uncertainty, the baseline should be increased.

The baseline distance must guarantee that on both the images there is a projection of the point M.

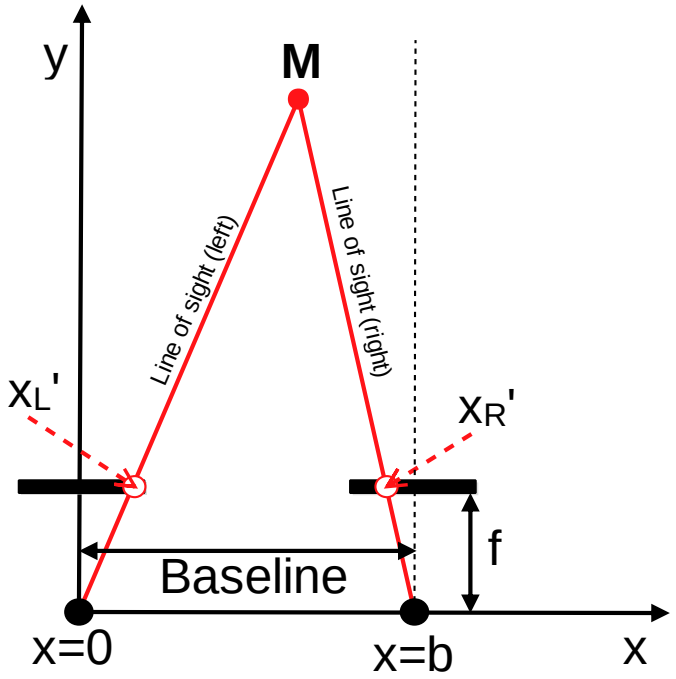

Depth measurement uncertainty

$$z = \frac{bf}{d}$$

By considering as unique uncertainty sources the disparity value and by applying the law of propagation of uncertainty, it is obtained:

$$u_z = \sqrt{\left(\frac{\partial z}{\partial d}\right)^2 u_d^2} = \frac{bf}{d^2} u_d \quad \text{, being } d = bf/z \quad \Rightarrow \quad u_z = \frac{z^2}{bf} u_d$$

- Disparity uncertainty = 1 pixel;
- 1 pixel size = 5 μm;
- Baseline = 1 m;
- Focal length = 10 mm.

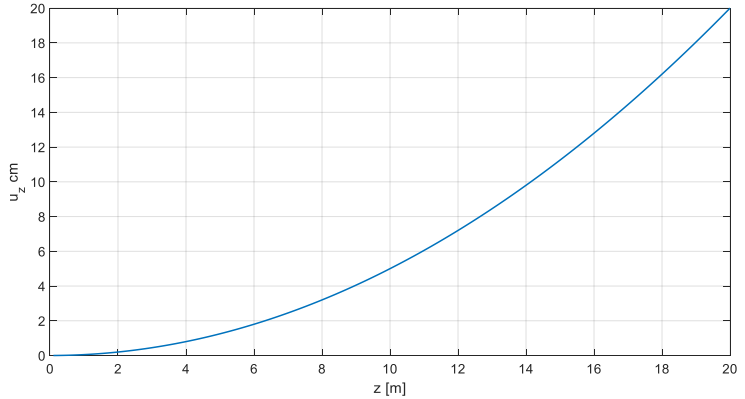

Metrological characterization of UAV aerial photogrammetry

Architectural overview of the proposed measurement analysis:

- The phase (1) shows the steps describing the independent observations on 3D maps created with Pix4Dmapper Pro and the developed 3D reconstruction tool.
- Phase (2) depicts the height uncertainty estimation process using the model that considers several measured quantities.
- In phase (3), the comparison between the uncertainty values provided by the three methods is shown.

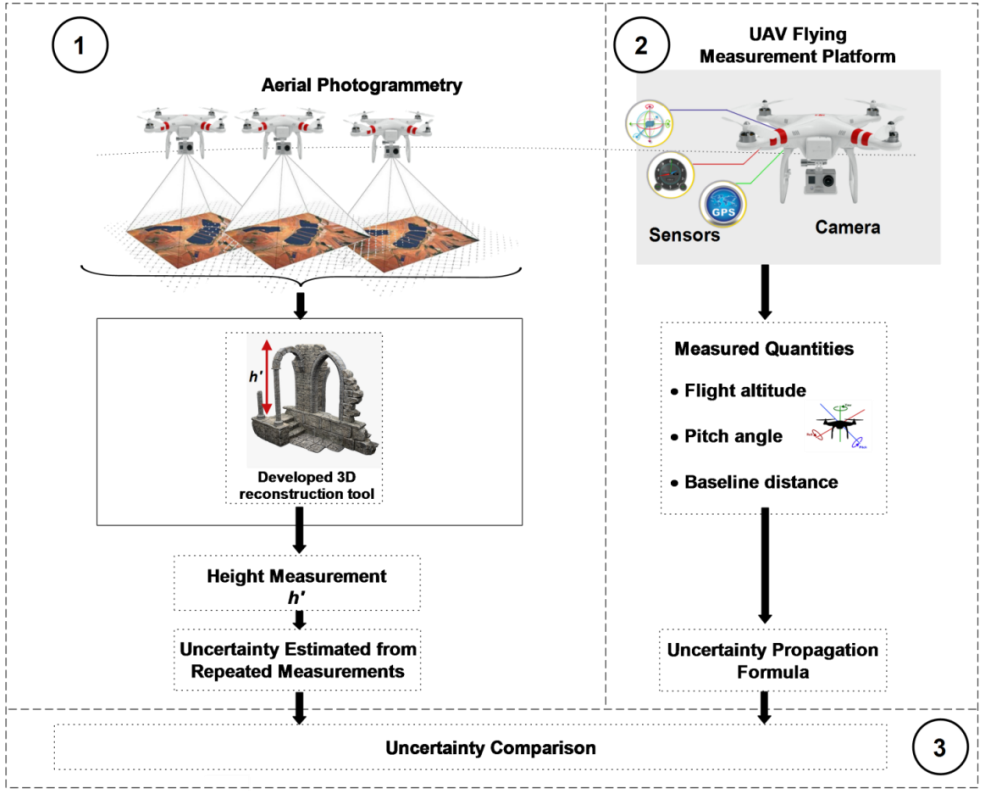

The advanced height measurement procedure (1)

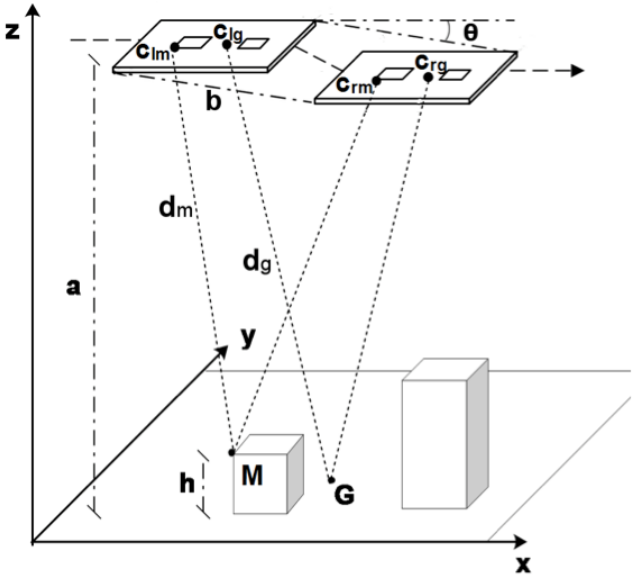

$$d_m = \left(\frac{c_{rm} \cdot \sin(q) - f \cdot \cos(q)}{f \cdot (c_{rm} - c_{lm})} \right) \cdot \left(f \cdot \cos(q) - c_{lm} \cdot \sin(q) \right) \cdot b$$

- d_m is the distance between the camera in the first waypoint and the point M;
- C_{lm} and C_{rm} are the pixel projections of the point M on the camera sensor array in both left and right positions;
- C_{lg} and C_{rg} are the pixel projections of the ground level point G on the camera sensor array;
- θ is the UAV elevation angle of drone in the second waypoint referred to the first;
- b is the distance between the positions related to image acquisitions;
- f is the camera focal length.

$$h = d_g - d_m = \left(\frac{c_{rm} \cdot \sin(q) - f \cdot \cos(q)}{f \cdot (c_{rm} - c_{lm})} \right) \cdot \left(f \cdot \cos(q) - c_{lm} \cdot \sin(q) \right) \cdot b - \left(\frac{c_{rg} \cdot \sin(q) - f \cdot \cos(q)}{f \cdot (c_{rg} - c_{lg})} \right) \cdot \left(f \cdot \cos(q) - c_{lg} \cdot \sin(q) \right) \cdot b$$

The advanced height measurement procedure (2)

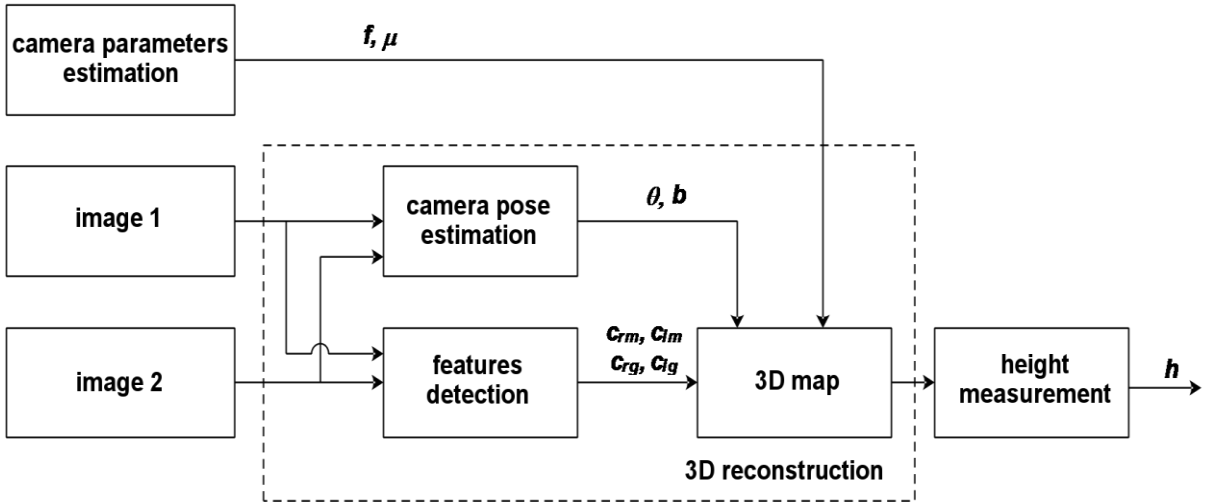

- The **Camera Parameters Estimation step** evaluates the internal quantities of the camera that affect the imaging processing.
- The **Camera Pose Estimation step** provides parameters referred to the stereovision geometry. This parameters can be evaluated using the measurements provided by sensors embedded on drones, e.g. GPS and IMU, or using image processing algorithms applied on the two acquired images.
- The **Features Detection step** selects a set of points whose coordinates (in pixels) can be identified on both images.

The proposed uncertainty model

$$u_h^2 = \left(\frac{dh}{dc_{rm}}\right)^2 \cdot u_{c_{rm}}^2 + \left(\frac{dh}{dc_{lm}}\right)^2 \cdot u_{c_{lm}}^2 + \left(\frac{dh}{dc_{rg}}\right)^2 \cdot u_{c_{rg}}^2 + \left(\frac{dh}{dc_{lg}}\right)^2 \cdot u_{c_{lg}}^2 + u_{cam}^2$$

This uncertainty model consists of two terms:

- the former one is due to the disparity values referred to the points M and G;
- the latter one takes into account the estimated stereovision geometry parameters and focal length

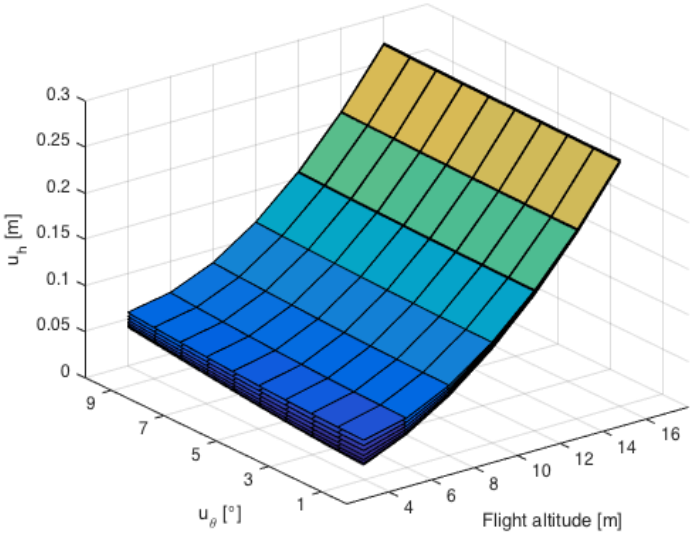

Uncertainty value [m] vs flight altitude [4, 16] m and pitch angle uncertainty value [1°, 10°], for different baseline uncertainty values [1.5, 10] cm

Experimental tests for Type A uncertainty evaluation

Pix4Dmapper Pro:

- Initial Processing, Pix4Dmapper Pro computes keypoints on the acquired images and provides a preliminary 3D map of the scene;
- Point Cloud and Mesh step increases the density of 3D points on the 3D map realized in Initial Processing step;
- Digital Surface Model (DSM) and Orthomosaic step provides a digital surface model and orthomosaic of the 3D map points. The 3D map can be scaled according to a reference size.

The developed 3D reconstruction application

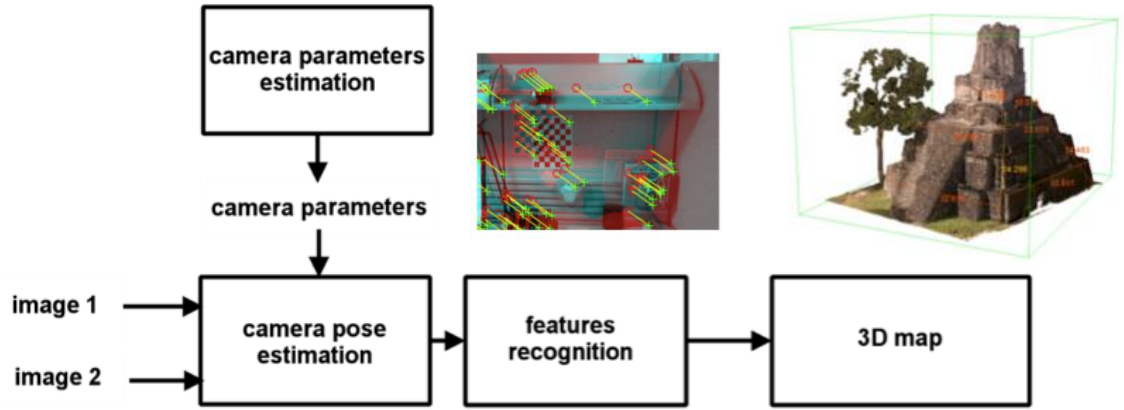

Repeatability Evaluation

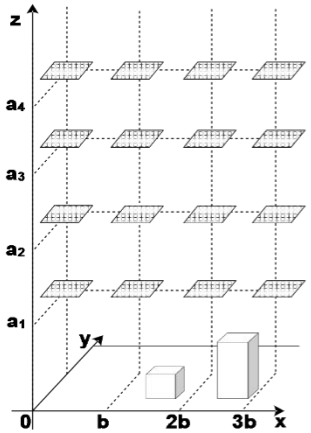

Camera parameters	Value
Number of effective pixels	12.4 megapixels
Field Of View	94° at 20 mm
Image Max Size	4000 x 3000 pixels
Sensor wide	6.16 mm
Sensor high	4.62 mm
Focal length	4 mm
Diagonal pixel sensor size	21.8 µm
ISO 5800:1987 range	100-1600

- For each position, 20 images have been acquired to evaluate the uncertainty related to each measurement.
- As target, a box has been used and its height of 0.418 m has been measured with the Leica Disto D3a infrared distance meter.
- For both the 3D reconstruction software, two averages of 6 distances camera-topside box (d_m) and 6 distances camera-ground level point (d_g) have been considered.
- The difference between these averaged values provides the object height measurement.
- An image scaling operation is performed in order to compensate systematic effects.

Results

Flight altitude [m]	3D application [m]	Proposed model [m]	Uncertainty of stereovision geometry parameters [m]	Pix4D [m]	Proposed model [m]	Uncertainty of stereovision geometry parameters [m]
3	0.20	0.20	0.20	0.25	0.24	0.24
7	0.12	0.11	0.10	0.45	0.44	0.44
9	0.17	0.16	0.13	0.43	0.43	0.42
11	0.23	0.22	0.18	0.30	0.29	0.26

- The main uncertainty sources for both the 3D reconstruction applications are due to the estimation of the stereovision geometry parameters;
- The uncertainty values related to the estimation of these stereovision parameters are higher for low flight altitudes than for the high ones. This is due to the fact that for low flight altitudes more details of the background are in the acquired images;
- The camera pose estimation algorithm is confused by the presence of more similar details on the background texture.

L.E.S.I.M. group

Prof. Pasquale Daponte

Prof. Sergio Rapuano

Prof. Luca De Vito

Prof. Francesco Lamonaca

Prof. Eulalia Balestrieri

Ioan Tudosa (Research fellow)

Francesco Picariello (Research fellow)

Gianluca Mazzilli (Research fellow)

Liliana Viglione (Research fellow)

Grazia Iadarola (Research fellow)

References

1) “Drones go to work”, available online: https://hbr.org/cover-story/2017/05/drones-go-to-work;
2) “4 Reasons Drones will revolutionize accident scene response”, available online: https://medium.com/the-science-of-drone-mapping/4-reasons-drones-will-revolutionize-accident-scene-response-a1db234eeccf;
3) K. P. Valavanis, G. J. Vachtsevanos, “Handbook of unmanned aerial vehicles”, Springer, 2014;
4) P. Daponte, L. De Vito, G. Mazzilli, F. Picariello, S. Rapuano, M. Riccio, “Metrology for drone and drone for metrology: measurement systems on small civilian drones”, Proc. of IEEE Workshop on Metrology for Aerospace, pp. 316-321, 3-5 June 2015, Benevento, Italy;
5) P. Daponte, L. De Vito, F. Picariello, S. Rapuano, M. Riccio, “An uncertainty model for height measurement based on aerial photogrammetry”, Proc. of 1st International Conference on Metrology for Archaeology, Benevento, Italy, October 22-23, 2015;
6) P. Daponte, L. De Vito, G. Mazzilli, F. Picariello and S. Rapuano, “A height measurement uncertainty model for archaeological surveys by aerial photogrammetry”, Measurement, Feb. 2017;
7) J. A. J. Berni, P. J. Zarco-Tejada, L. Suarez, and E. Fereres, “Thermal and narrowband multispectral remote sensing for vegetation monitoring from an Unmanned Aerial Vehicle,” IEEE Transaction On Geoscience and Remote Sensing, vol. 47, no. 3, pp. 722–738, 2009.
8) S. Burgos, M. Mota, D. Noll, and B. Cannelle, “Use of very high resolution airborne images to analyse 3D canopy architecture of a vineyard,” in The International Archives of the Photogrammetry, Remote Sensing and Spatial Information Sciences, 2015, pp. 399–403.
9) Gray A. Shaw and Hsiao-hua K. Burke, Spectral Imaging for Remote Sensing, Lincoln Laboratory Journal, vol. 14, No. 1, pp. 3-28, 2003.

Thank you for your attention!

L.E.S.I.M.
Laboratory of Measurement and Signal Processing
University of Sannio